ACS APPLIED MATERIALS & INTERFACES

Research Article

www.acsami.org

Nonvolatile Memory Thin-Film Transistors Using Biodegradable Chicken Albumen Gate Insulator and Oxide Semiconductor Channel on Eco-Friendly Paper Substrate

So-Jung Kim,[†] Da-Bin Jeon,[†] Jung-Ho Park,[†] Min-Ki Ryu,[‡] Jong-Heon Yang,[‡] Chi-Sun Hwang,[‡] Gi-Heon Kim,[‡] and Sung-Min Yoon*,[†]

[†]Department of Advanced Materials Engineering for Information and Electronics, Kyung Hee University, Yongin, Gyeonggi-do 446-701, Republic of Korea

[‡]Information & Communication Core Technology Research Laboratory, Electronics & Telecommunications Research Institute, Daejeon 305-730, Republic of Korea

Supporting Information

ABSTRACT: Nonvolatile memory thin-film transistors (TFTs) fabricated on paper substrates were proposed as one of the eco-friendly electronic devices. The gate stack was composed of chicken albumen gate insulator and In−Ga−Zn-O semiconducting channel layers. All the fabrication processes were performed below 120 °C. To improve the process compatibility of the synthethic paper substrate, an Al_2O_3 thin film was introduced as adhesion and barrier layers by atomic layer deposition. The dielectric properties of biomaterial albumen gate insulator were also enhanced by the preparation of Al_2O_3 capping layer. The nonvolatile bistabilities were realized by the switching phenomena of residual polarization within the albumen thin film. The fabricated device exhibited a counterclockwise hysteresis with a memory window of 11.8 V, high on/off ratio of approximately 1.1×10^6, and high saturation mobility (μ_{sat}) of 11.5 $cm^2/(V\ s)$. Furthermore, these device characteristics were not markedly degraded even after the delamination and under the bending situration. When the curvature radius was set as 5.3 cm, the I_{ON}/I_{OFF} ratio and μ_{sat} were obtained to be 5.9×10^6 and 7.9 $cm^2/(V\ s)$, respectively.

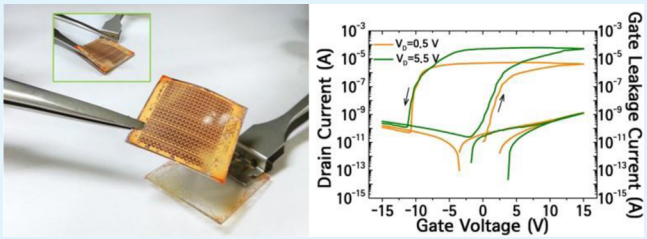

KEYWORDS: *eco-friendly device, nonvolatile memory, paper substrate, chicken albumen dielectric, oxide semiconductor*

1. INTRODUCTION

Environmental sustainability is one of the most critical demands for the next-generation electronic industries.[1,2] Therefore, high-performance electronic devices prepared on paper substrates have attracted huge interest as a promising technology to replace currently used plastic-based electronic devices. The mechanical features of the paper substrate also provide a higher degree of freedom in folding as well as in bending capability for flexible electronic systems.[3−5] Furthermore, the cost-effective and eco-friendly natures of the paper substrates secure the additional benefits. In recent days, various devices fabricated on paper substrates have been reported for their promising features such as low-voltage operation, low-power consumption, and data storage function.[6−10] However, the paper device performances were typically poor compared with those for the devices on glass or plastic substrate. Most biodegradable paper substrates suffer from several critical problems for electronic device applications such as water absorption, low heat resistance, and rough surface morphology. These limitations make it difficult to fabricate high-resolution thin-film transistor (TFT) arrays by using conventional photolithography and etching processes.[11] From these backgrounds, in this work, a synthetic paper, YUPO (synthesized by YUPO Corp.), made of polypropylene as a main ingredient, was chosen as a eco-friendly flexible substrate due to its high thermal durability and hydrophobic nature required for the wet-chemical-based full-patterning process using photolithography techniques. The choice of YUPO substrate is the first strategy of this work to solve the problems of conventional papers for the device fabrication and to improve the device characteristics through optimized fabrication procedures.

On the other hand, TFTs have been major workhorses for large-area electronics implemented on various substrates, and they can be played as switching and memory devices. It would be interesting to introduce eco-friendly biodegradable materials to device components such as the gate insulator (GI). Chicken albumen is one of the promising candidates. It can be easily and cheaply obtained from eggs without any additional process. The albumen layer can be comfortably formed by spin coating. The basic device characteristics for the oxide TFTs using chicken albumen gate dielectric were previously demonstrated.[11,12] In this work, we proposed the nonvolatile memory TFTs using

Received: December 15, 2014
Accepted: February 13, 2015
Published: February 13, 2015

DOI: 10.1021/am508834y
ACS Appl. Mater. Interfaces 2015, 7, 4869−4874

chicken albumen as a GI on the eco-friendly YUPO paper substrate. The memory TFT can also be an important element to realize highly functional future electronic systems composed of eco-friendly biodegradable devices. The nonvolatile bistability of the proposed memory TFT originated from the residual polarization effect of the albumen GI, which is analogous to the ferroelectric field-effect-driven memory transistor. This is the second strategy of this work to provide memory functions to the eco devices fabricated on the paper substrates. Thus, the main object of this work is to fabricate the reliable memory TFTs with the gate-stack structure of biodegradable albumen GI and oxide semiconductor channel on the eco-friendly YUPO paper substrate and demonstrate their nonvolatile memory performances. This is the first eco-paper memory TFT.

2. EXPERIMENTAL SECTION

A 300-μm-thick polypropylene-based synthetic paper YUPO (synthesized by YUPO) was chosen as a paper substrate. Compared with the conventional cellulose-based paper, it was featured to have a hydrophobic property and a better thermal stability. Thanks to these beneficial features, all the patterning processes for device fabrications could be carried out by conventional photolithography and wet-etching processes. As the first step, the YUPO substrate was laminated onto the glass substrate to facilitate the substrate handling. Then, a 3.6-μm-thick barrier layer (TR-8857-SA7, synthesized by Dongjin Semichem. Co. Ltd.) was spin-coated to reduce the surface roughness. A 30 nm-thick Al_2O_3 sample was deposited as an adhesion layer by atomic layer deposition (ALD), which was introduced to improve the adhesion between the organic barrier layer and source/drain (S/D) electrodes. A 150 nm-thick ITO was deposited by RF magnetron sputtering and patterned into the S/D electrodes. In−Ga−Zn-O (IGZO, 50 nm) was deposited as an active channel layer. Then, a 200 nm-thick diluted chicken albumen was spun at 4000 rpm for 30 s. Thermal treatment for curing and cross-linking were carried out at 120 °C for 10 min. Here, it was proposed to prepare an Al_2O_3 capping layer onto the albumen GI, which has important roles in protecting the albumen from the following patterning processes and in enhancing the adhesion between the gate electrodes. Finally, an Al film was deposited by thermal evaporation and patterned as gate electrodes and S/D pads. The electrical characteristics of the fabricated devices were evaluated by using a semiconductor parameter analyzer (Keithley 4200SCS) in a dark box at room temperature. Channel width and length of measured TFTs were 40 and 20 μm, respectively.

3. RESULTS AND DISCUSSION

3.1. Optimization of Fabrication Process for the Eco-Paper Memory TFTs. The fabrication process of diluted albumen solution is shown in Figure 1, panel a. The chicken white was separated and diluted by deionized water with a mixing ratio of 1:1. The precursor solution of albumen was finally prepared by stirring for 1 h at room temperature on a hot plate to obtain its homogeneity. Figure 1, panel b shows the polarization−electric field (P−E) characteristics of the fabricated Al/Al_2O_3/albumen/ITO capacitor. The top electrode diameter was 100 μm, and the signal frequency was 100 Hz. The remnant polarization (P_r) and the coercive field (E_c) were 0.97 μC/cm^2 and 1.2 MV/cm, respectively. It was suggested that residual polarization could be induced within the albumen film as if ferroelectric dipoles existed and that the nonvolatile bistability could be generated by remnant values of induced polarization for our proposed eco-paper memory TFT. To evaluate the effct of temperature on the protein denaturation of albumen and the corresponding P−E characteristics of the capacitors, the annealing temperature for the albumen was increased to 150 and 180 °C. As a result, the residual polarization dramatically disappeared when the albumen film was annealed above the temparture of 150 °C. Thus, the temperature of 120 °C, employed in this work, was concluded to be an optimum point for device fabrication and memory operations. The relative dielectric constant of the albumen layer was estimated from capacitance−frequency measurements to be approximately 15 at 1 MHz. Futhermore, we estimated the wettability of the albumen solution on YUPO (Figure 1c) and Al_2O_3-coated YUPO substrates (Figure 1d) by measuring the contact angles. As can be seen in the figure, the contact angle was reduced from 92.4 to 63.1° on the Al_2O_3-coated YUPO substrate. This result suggests that the wettability of the YUPO substrate to the albumen solution was significantly improved by suitability introducing the Al_2O_3 barrier layer.

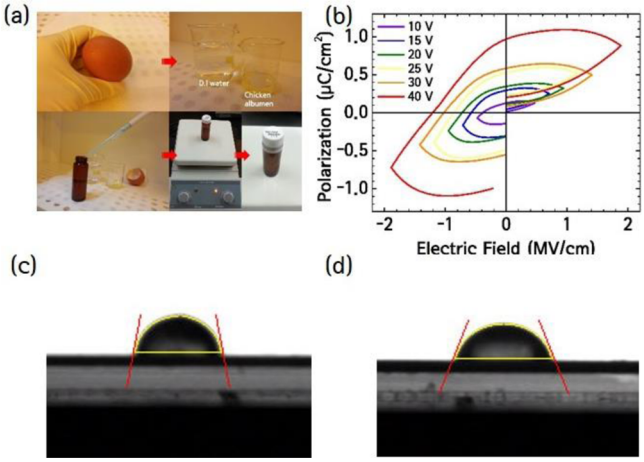

Figure 1. (a) Preparation procedures for diluted chicken albumen solution. (b) The polarization−electric field (P−E) characteristics of the fabricated Al/Al_2O_3/Albumen/ITO capacitor. The wettability of the albumen solution was examined on (c) YUPO substrate and (d) Al_2O_3-coated YUPO substrate by measuring the contact angle.

To fabricate the devices on YUPO substrate, the surface roughness should be carefully controlled. Figure 2, panel a shows the AFM images of the bare surface of YUPO substrate in which the arithmetic average of absolute roughness (R_a) value was approximately 22.3 nm, and surface morphology was rather inhomogeneous. Thus, the barrier layer was introduced to reduce the surface roughness. The R_a value for the barrier-coated substrate was markedly improved to 0.34 nm, as shown in Figure 2, panel b. The introduction of adhesion layer was also one of the most important features of the device fabrication process proposed in this work. Figure 2, panels c and d show the microscopic images for the situations of S/D patterning before and after the 30 nm-thick Al_2O_3 layer was prepared on the barrier layer, respectively. Sound patterns were obtained only on the adhesion layer. Figure 2, panels e−g show a schematic cross-section, cross-sectional SEM image, and optical microscope image of the fabricated albumen-paper memory TFT, respectively. The device was confirmed to be well fabricated, in which every layer composing the device configuration was obviously defined.

3.2. Device Characterizations for the Eco-Paper Memory TFTs. The capping layer (CL) of Al_2O_3 (10 nm) was prepared to protect the albumen GI during the fabrication process. The leakage current density of albumen layer was examined to be not so appropriate (3.2×10^{-5} A/cm^2 at 0.23

DOI: 10.1021/am508834y
ACS Appl. Mater. Interfaces 2015, 7, 4869−4874

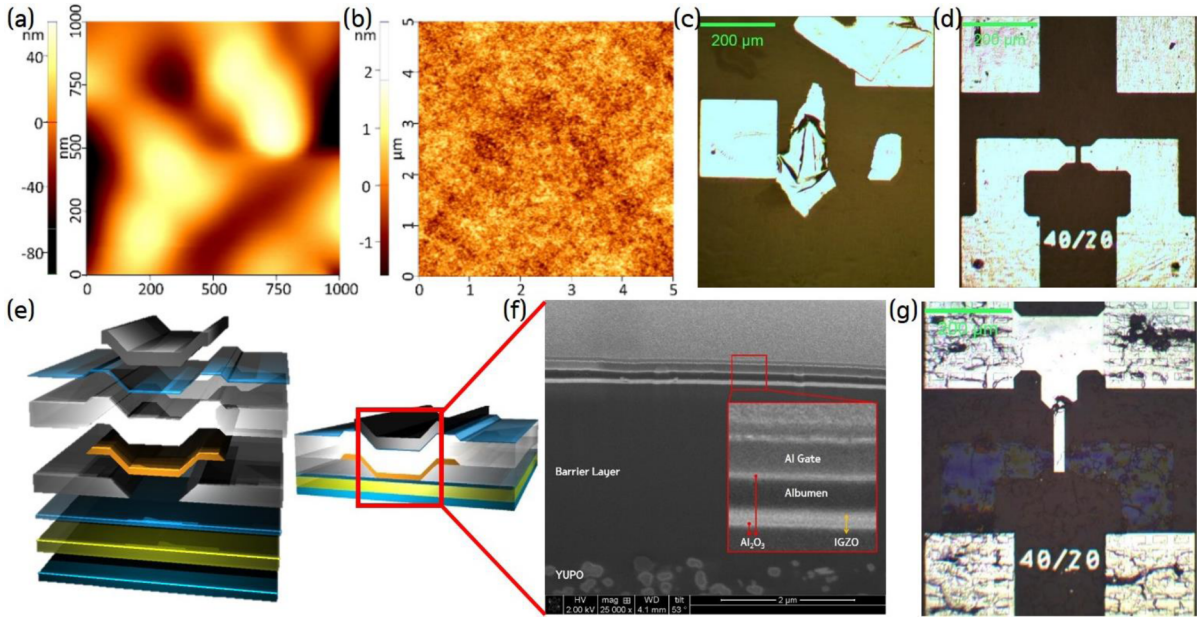

Figure 2. AFM images of the (a) bare and (b) barrier-coated surfaces of YUPO substrate. Microscopic images for the situations of S/D patterning (c) before and (d) after deposition of 30 nm-thick Al_2O_3 layer. (e) Schematic cross-section, (f) cross-sectional SEM image, and (e) optical microscope image of the fabricated eco-paper memory TFT.

MV/cm) for the GI application, and it was additionally degraded after the wet process using a resist stripper, as shown in Figure 3, panel a. On the contrary, the CL-treated albumen layer exhibited excellent insulating characteristics, in which the leakage current densities were effectively suppressed to 9.0×10^{-9} and 5.5×10^{-8} A/cm^2 before and after the resist strip process, respectively. The introduction of the CL was clearly found to have beneficial impact in enhancing the dielectric insulation property and protecting from the chemical damages for the albumen layer. Figure 3, panel b shows the drain current−gate voltage ($I_{DS} - V_{GS}$) characteristics and gate leakage currents of the fabricated eco-paper memory TFT with the gate width and length of 40 and 20 μm. Transfer characteristics were measured in the double sweep mode of V_{GS} from −20−20 V at V_{DS} of 0.5 and 5.5 V. We calculated the device parameters by using accumulation capacitance values measured at 10 kHz, as shown in Figure 3, panel c. Although off-current levels were relatively high, the on/off switching behavior could be clearly obtained. The I_{on}/I_{off} ratio was approximately 1.1×10^6. The saturation mobility (μ_{sat}) and threshold voltage (V_{TH}) were evaluated to be 11.5 cm^2/(V s) and 2.5 V, respectively, which were calculated from the derivative and x-axis intercept of $(I_{DS})^{0.5} - V_{GS}$ plot using the standard saturation current equation. The subthreshold swing (S.S) value was also estimated to be 1.03 V/dec. It was interesting to note that wide counterclockwise hysteresis in I_{DS} was observed due to the remnant polarization of albumen GI. The memory window (MW), which was determined as the voltage width between turn-on and turn-off points, was estimated to be approximately 11.8 V. These results demonstrated a feasibility that the fabricated device could exhibit nonvolatile memory characteristics by exploiting the effect of residual polarization within the albumen GI, as expected in P−E characteristics (Figure 1a).

The capacitance−voltage (C−V) characteristics were also examined, as shown in Figure 3, panel c. Grounding the S/D terminals, V_{GS} was swept from −30−15 V in forward and

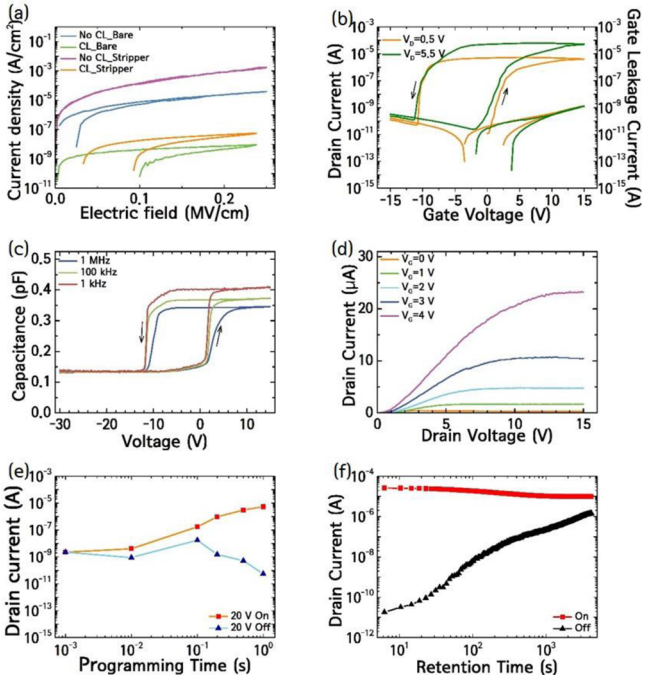

Figure 3. (a) Leakage current densities of albumen and CL-treated albumen layers with and without treatments in resist stripper. (b) $I_{DS} - V_{GS}$ characteristics and gate leakage currents of the fabricated device with the W/L of 40/20 μm. Transfer curves were measured in the double sweep mode of V_{GS} from −15−15 V at V_{DS} of 0.5 and 5.5 V. (c) C−V measurements for the fabricated device. Grounding S/D terminals, V_{GS} was swept from −30−15 V. The measurement frequency was varied to 1 MHz, 100 kHz, and 10 kHz, respectively. (d) $I_{DS} - V_{DS}$ output characteristics at different V_{GS} values from 0−4 V in steps of 1 V. (e) Variations in the programmed I_{DS} of the fabricated eco-paper memory TFT when the pulse widths of program voltages for on and off were varied from 1 ms to 1 s with the voltage amplitude of 20 and −20 V, respectively. (f) The variations in the programmed I_{DS} with the lapse of retention time of 4×10^3 s.

DOI: 10.1021/am508834y
ACS Appl. Mater. Interfaces 2015, 7, 4869−4874

reverse directions. The measurement frequency was varied to 1 MHz, 100 kHz, and 10 kHz. Although the accumulation capacitance values decreased with the increase in frequency due to the frequency dispersion, the MW was almost maintained even at 1 MHz. The nonvolatile memory characteristics were also verified in C−V measurements for the fabricated eco-paper memory TFT. Figure 3, panel d shows the typical output characteristics ($V_{DS} - I_{DS}$) at different gate voltages (V_{GS}) from 0−4 V in steps of 1 V. As can be seen in the figure, the eco-paper memory TFT exhibited good gate modulation and hard saturation behaviors for the saturation region, although a current crowding behavior was observed in the linear region, which indicates a moderately high contact resistance between the S/D and active layers, which probably originated from the thermal deformation of YUPO substrate during the processes. It happens that the trap or defect sites exist at IGZO interfaces or within bulk films of IGZO and albumen layers. However, for *n*-type devices, counterclockwise and clockwise directions of hysteresis in transfer curves represent the residual polarization and charge injection mechanisms, respectively, as a dominant effect causing the hysteretic behaviors. For our fabricated eco-paper memory TFTs, the direction of hysteresis was observed to be counterclockwise, as shown in Figure 3, panel b. Therefore, we can exclude the possibility of charge-trap mechanism. It would be very important to check the origin of the obtained counterclockwise hysteresis shown in Figure 3, panels b and c because they might also be caused by mobile ions with which the nonvolatile memory switching cannot be guaranteed for practical applications. To analyze these behaviors, the memory programming characteristics were verified by voltage pulse signals with given duration. Figure 3, panel e shows the variations in the programmed I_{DS} of the fabricated eco-paper memory TFT when the pulse widths of program voltages applied for on and off programming were varied from 1 ms to 1 s at voltage amplitude of 20 and −20 V, respectively.

While the program operations could not be achieved for the cases using pulses shorter than 100 ms, the memory on/off ratio significantly increased with increased pulse width from 100 ms to 1 s. The eco-paper memory TFT exhibited the maximum memory on/off ratio of approximately 1.0×10^6. Consequently, it was clearly suggested that the polarization effects within the chicken-albumen GI induced the hysteretic bistability observed in the fabricated device. These results demonstrated that our proposed eco-paper memory TFT could be operated as promising nonvolatile memory TFT. In most practical memory applications, the stored data should be retained with the lapse of time. Thus, to examine the data retention characteristics, ± 20-V-high and 1-s-wide programming pulses were applied, and the programmed I_{DS} was measured at a read-out V_{GS} of 0 V. Figure 3, panel f shows the variations in the programmed on and off I_{DS} with the lapse of retention time of 4×10^3 s. The on/off ratio was initially obtained to be approximately 1.4×10^6 and decreased to 4.8 after 1000 s. It was found that the memory off-state was more markedly varied with the retention time than the memory on-state. This asymmetric increase of off-programmed current can be interpreted by the depolarization field asymmetrically determined between the on and off states. Because the *n*-ch IGZO TFT operates in a depletion mode for the memory off-state, the depolarization field applied for the off-state during the retention period is subject to be larger than that for the on-state. Thus, a larger degradation may occur for the off-programmed state.[13] This problem could be improved by appropriate device designs including the film thicknesses of active channel, gate insulator, and capping layers. Even though the retention time for this device was not so long at this stage, the presented nonvolatile memory behaviors of the eco-paper memory TFT could be sufficiently encouraging for future biodegradable−flexible memory applications. Concerning the yield and uniformity in device behaviors, the number of working devices amounted to ten when the test patterns were designed to have 20 TFTs with the same size in a single device substrate. The yield would be enhanced by further improvements in fabrication process. When examined with ten working devices as the average performances, the memory window and the I_{ON}/I_{OFF} were estimated to be approximately 12.7 ± 1.3 V and $4.0 \times 10^6 \pm 2.6 \times 10^6$, respectively.

In practical applications, the YUPO substrate attached on the glass substrate for easy handling during the process should be delaminated, and the device characteristics of the delaminated paper memory TFT should be evaluated again. Figure 4, panel a shows the photo images of the fabricated devices on the YUPO substrate delaminated from the glass substrate. The delamination was easily performed by using tweezers wetted with acetone, as shown in inset of Figure 4, panel a. As shown in Figure 4, panel b, the detached device did not experience marked mechanical deformation or peel-off of given layers composing the device. Figure 4, panel c shows the transfer characteristics of the eco-paper memory TFT after the delamination. The I_{ON}/I_{OFF} ratio was obtained as 0.4×10^6 at V_{DS} of 0.5 V. The μ_{sat}, V_{TH}, and S.S values were estimated to be 6.3 $cm^2/(V\,s)$, 4.7 V, and 0.70 V/dec, respectively. Although the μ_{sat} was degraded owing to the mechanical damage during the delamination process, the obtained device behaviors were quite inspiring, considering that the devices were fabricated on a flexible paper substrate. The memory programming properties were also examined, as shown in Figure 4, panel d.

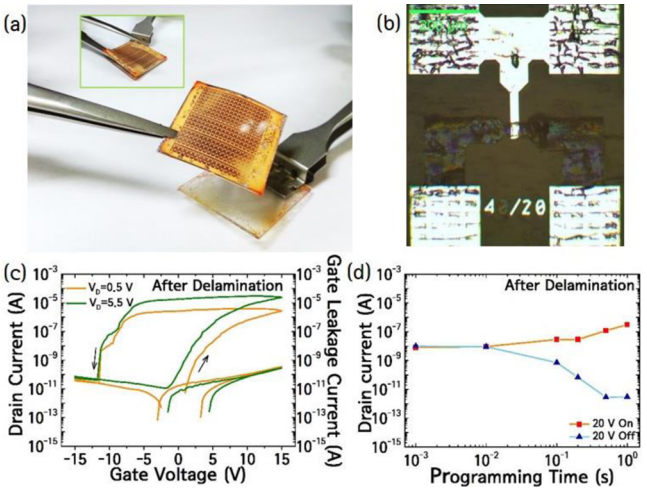

Figure 4. (a) Photo and (b) microscopic images of the devices fabricated on the YUPO substrate delaminated from the glass substrate. (c) Transfer characteristics of the eco-paper memory TFT after the delamination. (d) Memory programming properties of the delaminated memory transistor when the pulse widths of program voltages were varied from 1 ms to 1 s. The program voltages for the memory on and off states were ±20 V.

The variations in the memory on/off ratio as a function of program pulse width were not so different from those for the

DOI: 10.1021/am508834y
ACS Appl. Mater. Interfaces 2015, 7, 4869−4874

laminated device, and the maximum memory on/off ratio of 1.0 × 10^5 was obtained. These results suggested that the proposed memory TFT fabricated on the paper substrate can be operated in a stand-alone manner without any supporting substrate.

For the flexible memory applications, the variations in device behaviors against mechanical bending deformation must be estimated for the fabricated memory TFT. The probing configuration for the bending durability test can be shown in Figure 5, panel a. Figure 5, panel b shows the bending

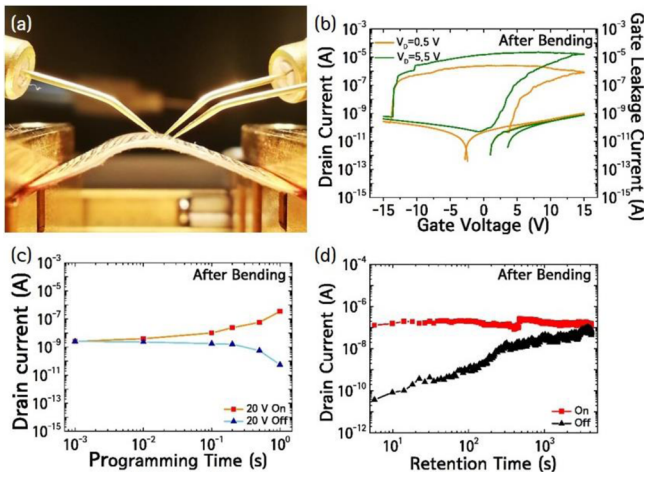

Figure 5. (a) Photo image of an electrical evaluation and (b) transfer characteristics for the fabricated device under the bending situation. (c) Memory programming and (d) retention properties were also evaluated under the bending situation.

characteristics of the eco-paper memory TFT by measuring the transfer characteristics and gate leakage currents when the substrate was bent with a curvature radius of 5.3 cm. The I_{ON}/I_{OFF} ratio was obtained as 5.9 × 10^6 at V_{DS} of 0.5 V. The μ_{sat}, V_{TH}, and S.S values were examined to be 7.9 $cm^2/(V\ s)$, 9.1 V, and 0.77 V/dec, respectively. Although the device operation behaviors under the bending situations were slightly changed compare with those of the delaminated device, the obtained device parameters including the μ_{sat} did not show any marked degradation. Memory programming operation and retention characteristics were also examined, as shown in Figure 5, panels c and d, respectively. The maximum memory I_{ON}/I_{OFF} ratio was obtained as 6.3 × 10^3 at 1-s-width programming signals. The programmed initial I_{ON}/I_{OFF} ratio of 3.4 × 10^3 decreased to 2.2 after the lapse of 4 × 10^3 s. The nonvolatile memory behaviors examined under the bending situations were sufficiently encouraging. The reproducibility and stability in electrical performance of the proposed eco-paper memory TFTs could be guaranteed by the fabrication process optimizations, as discussed above, and are sufficiently reliable at a present stage.

4. CONCLUSION

We proposed and fabricated the nonvolatile memory TFTs using biomaterial, chicken albumen, as GI on eco-friendly paper substrate for the first time. All components were elaborately patterned with photolithography techniques, and all fabrication processes were performed at low temperature below 120 °C. For the use of albumen as GI, the dielectric properties were enhanced by the introduction of Al_2O_3 capping layer. The nonvolatile bistability for memory operations was realized by the switching phenomenon of residual polarization in the albumen GI. The fabricated eco-paper memory TFT exhibited high mobility (~11.5 $cm^2/(V\ s)$) and high I_{ON}/I_{OFF} ratio (>10^6) thanks to the optimization of fabrication procedures. Good programming operations and memory retention performances were also successfully confirmed, in which the maximum I_{ON}/I_{OFF} ratio of 1.0 × 10^6 was obtained with 1-μs-wide program pulse of ±20 V. Furthermore, these device characteristics were not markedly degraded even after the delamination and under the bending situation. When the curvature radius was set as 5.3 cm, the I_{ON}/I_{OFF} ratio, μ_{sat}, V_{TH}, and S.S values were examined to be 5.9 × 10^6, 7.9 $cm^2/(V\ s)$, 9.1 V, and 0.77 V/dec, respectively. These inspiring and encouraging results obtained from the proposed eco-paper memory TFTs are expected to find new possibilities in the fields of future sustainable electronics.

■ ASSOCIATED CONTENT

Supporting Information

Associated content including (i) the output characteristics (I_{DS} − V_{DS}) and C−V characteristics after the delamination and under the bending situation, (ii) the process compatibility and effects of capping layer on the insulating properties of albumen, (iii) the annealing temperature dependence of the residual polarization effect of chicken albumen thin films, (iv) the adhesion improvement by the introduction of barrier layer, and (v) the suitability to the environmental needs evaluated in burning state. This material is available free of charge via the Internet at http://pubs.acs.org.

■ AUTHOR INFORMATION

Corresponding Author

*Phone: 82-31-201-3617. Fax: 82-31-204-8114. E-mail: sungmin@khu.ac.kr.

Notes

The authors declare no competing financial interest.

■ ACKNOWLEDGMENTS

This research was supported by the National Research Foundation of Korea (NRF) grant funded by the Korean government (MEST) (2014063718). This research was also funded by the MSIP (Ministry of Science, ICT & Future Planning), Korea in the ICT R&D Program (the core technology development of light and space adaptable energy-saving I/O platform for future advertising service).

■ REFERENCES

(1) Martins, R.; Barquinha, P.; Pereira, L.; Correia, N.; Gonçalves, G.; Ferreira, I.; Fortunato, E. Write−Erase and Read Paper Memory Transistor. *Appl. Phys. Lett.* **2008**, *93*, 203501.

(2) Siegel, A. C.; Phillips, S. T.; Wiley, B. J.; Whitesides, G. M. Thin, Lightweight, Foldable Thermochromic Displays on Paper. *Lab Chip* **2009**, *9*, 2775−2781.

(3) Lim, W.; Douglas, E. A.; Kim, S. H.; Norton, D. P.; Pearton, S. J.; Ren, F.; Shen, H.; Chang, W. H. High Mobility $InGaZnO_4$ Thin-Film Transistors on Paper. *Appl. Phys. Lett.* **2009**, *94*, 072103.

(4) Lu, A.; Dai, M.; Sun, J.; Jiang, J.; Wan, Q. Flexible Low-Voltage Electric-Double-Layer TFTs Self-Assembled on Paper Substrates. *IEEE Electron Device Lett.* **2011**, *32*, 518−520.

(5) Russo, A.; Ahn, B. Y.; Adams, J. J.; Duoss, E. B.; Bernhard, J. T.; Lewis, J. A. Pen-on-Paper Flexible Electronics. *Adv. Mater.* **2011**, *23*, 3426−3430.

(6) Li, Y.; Li, C.; Xu, Y.; Minari, T.; Darmawan, P.; Tsukagoshi, K. Solution-Processed Organic Crystals for Field-Effect Transistor Arrays

DOI: 10.1021/am508834y
ACS Appl. Mater. Interfaces 2015, 7, 4869−4874

with Smooth Semiconductor/Dielectric Interface on Paper Substrates. *Org. Electron.* **2012**, *13*, 815−819.
(7) Lien, D. H.; Kao, Z. K.; Huang, T. H.; Liao, Y. C.; Lee, S. C.; He, J. H. All-Printed Paper Memory. *ACS Nano* **2014**, *8*, 7613−7619.
(8) Lim, W.; Douglas, E. A.; Norton, D. P.; Pearton, S. J.; Ren, F.; Heo, Y. W.; Son, S. Y.; Yuh, J. H. Low-Voltage Indium Gallium Zinc Oxide Thin Film Transistors on Paper Substrates. *Appl. Phys. Lett.* **2010**, *96*, 3510.
(9) Khanna, R.; Douglas, E. A.; Norton, D. P.; Pearton, S. J.; Ren, F. Ti/Au Ohmic Contacts to Indium Zinc Oxide Thin Films on Paper Substrates. *J. Vac. Sci. Technol., B* **2010**, *28*, L43−L46.
(10) Mazzeo, A. D.; Kalb, W. B.; Chan, L.; Killian, M. G.; Bloch, J. F.; Mazzeo, B. A.; Whitesides, G. M. Paper-Based, Capacitive Touch Pads. *Adv. Mater.* **2012**, *24*, 2850−2856.
(11) Jeon, D. B.; Bak, J. Y.; Yoon, S. M. Oxide Thin-Film Transistors Fabricated Using Biodegradable Gate Dielectric Layer of Chicken Albumen. *Jpn. J. Appl. Phys.* **2013**, *52*, 128002.
(12) Chang, J. W.; Wang, C. G.; Huang, C. Y.; Tsai, T. D.; Guo, T. F.; Wen, T. Chicken Albumen Dielectrics in Organic Field-Effect Transistors. *Adv. Mater.* **2011**, *23*, 4077−4081.
(13) Yoon, S.; Yang, S.; Park, S.; Jung, S.; Cho, D.; Byun, C.; Kang, S.; Hwang, C.; Yu, B. Effect of ZnO Channel Thickness on the Device Behavior of Nonvolatile Memory Thin Film Transistors with Double-Layered Gate Insulators of Al_2O_3 and Ferroelectric Polymer. *J. Phys. D: Appl. Phys.* **2009**, *42*, 245101.

DOI: 10.1021/am508834y
ACS Appl. Mater. Interfaces 2015, 7, 4869−4874